

Supplementary Material

Interrupting the nitrosative stress fuels tumour-specific cytotoxic T lymphocytes in pancreatic cancer

Francesco De Sanctis, Alessia Lamolinara, Federico Boschi, Chiara Musiu, Simone Caligola, Rosalinda Trovato, Alessandra Fiore, Cristina Frusteri, Cristina Anselmi, Ornella Poffe, Tiziana Cestari, Stefania Canè, Silvia Sartoris, Rosalba Giugno, Giulia Del Rosario, Barbara Zappacosta, Francesco Del Pizzo, Matteo Fassan, Erica Dugnani, Lorenzo Piemonti, Emanuela Bottani, Ilaria Decimo, Salvatore Paiella, Roberto Salvia, Rita T. Lawlor, Vincenzo Corbo, Youngkyu Park, David A. Tuveson, Claudio Bassi, Aldo Scarpa, Manuela Iezzi, Stefano Ugel and Vincenzo Bronte.

Corresponding authors:

Prof. Vincenzo Bronte

University Hospital and Department of Medicine, Immunology Section, Verona, Italy.

Phone: +39-045-8126451;

Fax: +39-045-8126455;

E-mail: vincenzo.bronte@univr.it

Dr. Francesco De Sanctis

University Hospital and Department of Medicine, Immunology Section, Verona, Italy.

Phone: +39-045-8126454;

Fax: +39-045-8126455;

E-mail: francesco.desanctis@univr.it

This PDF file includes:

Supplementary Materials and Methods

References

Supplementary Figures 1-9

Supplementary Figure legends

SUPPLEMENTARY METHODS

Cell culture

Mouse FC1199 (H-2^b) and FC1242 (H-2^b) KPC-derived cell lines were kindly supplied by Dr. D. Tuveson (Cold Spring Harbor Laboratory, NY, USA); MBL-2 (H-2^b) mouse cells were kindly provided by Dr. James C. Yang (National Institutes of Health, Bethesda, MD). Cell lines were cultured in Dulbecco's modified Eagle's medium (DMEM) supplemented with 10% heat-inactivated FBS (Superior, Merck, Darmstadt, Germany), 2mM L-glutamine, 10mM HEPES and 200U/mL penicillin/streptomycin (all purchased from Euroclone, Milan, Italy). FC1199-Luc and FC1242-Luc were generated by transduction with a lentivirus built up with the pLENTI.EGFP.Luc vector. FC1199-Luc and FC1242-Luc cells were generated by infection with a firefly luciferase-EGFP coding lentivirus and enriched by FACS-Aria to get EGFP⁺ fraction higher than 95%.

Human HLA-A2 restricted PANC-1 (CRL-1469), HPAF-II (CRL-1997), CFPAC-1(CRL-1918), MiaPaca2(CRL-1420), T2 (174 x CEM.T2) cell lines were purchased from ATCC (Mannas, USA), whereas PT-45, PaCa-44, GER, T3M4, HF2 cell lines were kindly supplied by Dr. A. Scarpa and Dr. V. Corbo (University of Verona, Verona, Italy). All the human PDAC cell lines were cultured in RPMI-1640 supplemented with 2mM L-glutamine, 10mM HEPES, 1mM sodium pyruvate (all purchased from Euroclone, Milan, Italy), 200U/mL penicillin/streptomycin and 10% heat-inactivated FBS. Cell lines were thawed from primary stocks maintained under liquid nitrogen and cultured for a maximum of 1 month during which time all experiments were performed. The cultures were maintained at 37°C in 5% CO₂-humidified atmosphere and regularly tested for Mycoplasma using MycoAlert LookOut Mycoplasma PCR Detection Kit (Sigma-Aldrich, Saint Louis, MO, USA).

Polyclonal mTERT₁₉₈₋₂₀₅ CTLs were obtained from a mixed-leukocyte peptide culture set up with vaccinated mice splenocytes in presence of 0.1 μM of mTERT₁₉₈₋₂₀₅ peptide (VGRNFTNL) [1]. Cells were maintained by co-culture with irradiated, syngenic splenocytes pulsed with 0.1 μM TERT peptide in complete medium containing 20 IU/mL of recombinant human IL-2 (Miltenyi Biotec, Germany). OVA₂₅₇₋₂₆₄-specific CTLs derived from OT-1 splenocytes were stimulated once with 1 μM specific OVA (SIINFEKL) peptide in complete medium containing 20 IU/mL of recombinant human IL-2 (Miltenyi Biotec, Germany; Cat# 130-097-748) were used as control.

hTERT₈₆₅₋₈₇₃-specific TCR sequences were isolated as previously described [2]. As control, T lymphocyte engineered with a transgenic TCR specific for epitope hHCV₁₄₀₆₋₁₄₁₅ (KLVALGINAV) were generated. hTERT₈₆₅₋₈₇₃- and hHCV₁₄₀₆₋₁₄₁₅- specific T lymphocytes were produced by transduction of activated PBMCs with the viral supernatant of hTERT₈₆₅₋₈₇₃- or hHCV₁₄₀₆₋₁₄₁₅- PG13 cell lines in the presence of recombinant human (rh) IL-15 (100 μg/mL, Miltenyi Biotec, Germany; Cat#170-076-114) and rIL-2 (300 IU/mL, Miltenyi Biotec, Germany; Cat# 130-097-748). Selected T lymphocytes were then expanded in AIM-V medium (Gibco, Thermo Fisher Scientific, Waltham, MA, USA) supplemented with 5% human serum (Gibco, Thermo Fisher Scientific, Waltham, MA, USA) with anti-CD3 (clone OKT-3;30 ng/mL; eBioscience, Thermo Fisher Scientific, Waltham, MA, USA; Cat#16-0037-85), rhIL-2 and rhIL-15. In general, CD8⁺ T lymphocytes represent about 70-80% of the total T lymphocytes culture and numbers for *in vivo* treatments were adjusted in order to inject 8x10⁶ CTLs.

Synthetic peptides and reagents

H-2K^b-restricted OVA peptide (OVA₂₅₇₋₂₆₄, SIINFEKL), H-2K^b-restricted peptide mTERT₁₉₈₋₂₀₅ (VGRNFTNL), HLA-A2-restricted hTERT₈₆₅₋₈₇₃ peptide (RLVDDFLLV) and HLA-A2-restricted hHCV₁₄₀₆₋₁₄₁₅ (KLVALGINAV) peptide were all synthesized by JPT (JPT, Peptide Technologies,

Germany). For *in vivo* treatment, AT38 was dissolved in 1% carboxymethylcellulose in sterile saline solution and intraperitoneally (i.p.) injected.

Telomerase activity

Telomerase activity was assessed on cell extracts by TRAP assay (TRAPeze® telomerase detection kit; Millipore, Merck, Darmstadt, Germany, Cat# S7710), a sensitive and efficient PCR-based telomerase activity detection method following manufacturer's instructions. Briefly, 5×10^5 cell pellets were lysed and proteins extracted in CHAPS buffer for 30' in ice. After centrifugation the supernatant was collected and split in half. One part was heat treated to denature Telomerase (negative control used to prove the specificity of the recorded signals), the other (testing condition) was kept on ice. Positive and negative samples were all subjected to real time PCR which amplifies telomeres tandem repeats generated in the first step of the reaction by TERT activity. Thus, the recorded signal is proportional to TERT activity. In the same assay, a titration curve is generated in order to quantify TERT activity.

Preparation of cell suspensions from mouse organs

Spleens and tumours were collected from euthanized mice and processed according to already published protocols [3]. Briefly, spleens were mechanically disaggregated, washed, deprived by red blood cells and filtered on cell strainer (Corning Inc, New York, USA) to remove aggregates. Tumours were finely minced and enzymatically digested with a solution containing collagenase IV (1 mg/ml; Cat# C4-28), hyaluronidase (0.1 mg/mL; Cat# HX0514) and DNase (4.5 mg/mL; Cat# D4263) (all from Sigma-Aldrich, Saint Louis, MO, USA) for 1 hour at 37°C. During this incubation samples were mechanically disaggregated twice with 2 ml needle-less syringe. Tumour cells suspension was separated from aggregates by cell strainer filtration, washed with complete DMEM media and, if necessary, deprived by red blood cells. Finally, cells were utilized for *in vitro* testing or immunomagnetic sorting.

Preparation of tumour conditioned media

For *ex-vivo* protein profile, cell suspensions derived from naïve pancreata or orthotopic tumours were plated at a concentration of 1×10^6 cells/ml (2ml of complete DMEM media) in a 6 well plate and cultured for 48 hours. For *in vitro* protein profile, tumour cells were plated at 2.5×10^5 cells/ml (2ml of complete DMEM media) in a 6 well plate and cultured for 48 hours. Conditioned media were collected, centrifuged and analysed by ELISA in order to quantify CCL2, GM-CSF, IL-6, IL-10, VEGF cytokines (all purchased from Affymetrix Santa Clara, California, USA).

Immunomagnetic sorting

CD11b⁺ cells were isolated from spleens and tumours with anti-CD11b MicroBeads (Miltenyi Biotec, Germany; Cat# 130-126-725). All separations were performed according to manufacturer's instructions by using Midi Macs columns (Miltenyi Biotec, Germany; Cat# 130-042-401). Purity of cell populations was evaluated by flow cytometry and exceeded 90%.

Ex vivo T lymphocyte suppression assays

CD11b⁺ cells-dependent suppression of T lymphocyte proliferation and killing activity were evaluated accordingly to recent published protocols [4]. Briefly in T lymphocyte proliferation assay, CD11b⁺ cells were added at various percentages (from 24% to 3% of total cells) to 1 μ M Celltrace- or 1 μ M Carboxyfluorescein succinimidyl ester (CFSE) (Thermo Fisher Scientific, Waltham, MA, USA; Cat# C34557) labelled CD45.2 OT1 splenocytes (previously diluted 1:10 with CD45.1⁺ splenocytes) in the presence of OVA₂₅₇₋₂₆₄ peptide (1 μ g/ml final concentration). After 3 days of co-

culture, cells were stained with anti-CD45.2⁺ and anti-CD8 and CellTrace signal of gated lymphocytes was measured. The percentage of suppression was calculated with the following formula: $[1 - (\% \text{ divided cells in sample} / \% \text{ divided cells in activated control})] \times 100$.

In Chromium release assay, a mixed leukocyte peptide culture (MLPC) was established using OT1 splenocytes stimulated for 4 days with OVA₂₅₇₋₂₆₄ peptide in presence of decreasing percentages (from 24% to 3% of total cells) of CD11b⁺ cells isolated from tumour or spleen of tumour-bearing mice. After 4 days, MLPCs were counted and co-cultured at different ratios with target (MBL-2) cells, previously pulsed with OVA₂₅₇₋₂₆₄ or scramble peptide (1 µg/mL) and hexavalent chromium-51 (⁵¹Cr – Beckman Coulter, Brea, California, USA). After 5 hours of incubation at 37°C supernatant was transferred on Luma Plates (Perkin Elmer, Waltham, MA, USA) and ⁵¹Cr measured by TopCount device (Perkin Elmer, Waltham, MA, USA). The % of lysis was calculated using the formula:

$$\% \text{ lysis} = (\text{cpm}^{\text{experimental}} - \text{cpm}^{\text{spontaneous}}) / (\text{cpm}^{\text{maximum}} - \text{cpm}^{\text{spontaneous}}) \times 100.$$

Flow cytometry

1x10⁶ cells were incubated with Fc Receptor Blocking reagent CD16/32 (Biolegend, San Diego, CA, USA; Cat# 101302) for 10 minutes at 4°C to saturate FcRs. The following mAbs were then used for cell labelling: anti-mouse B220 (RA3-6B2; Cat#25-0452-82), CD11b (M1/70; Cat# 101228), CD11c (N418; Cat# 17-0114-82), CD3 (17A2; Cat# 100222), CD4 (GK1.5; Cat# 45-0042-82), CD44 (IM7; Cat# 103043), CD45 (30F-11; Cat# 103138), CD45.1 (A20; Cat# 110708), CD45.2 (104; Cat# 109814), CD62L (MEL14; Cat# 47-0621-82), CD8 (53-6.7; Cat# 11-0081-82), F4/80 (CL:A3-1; Cat# MCA497R), Ly6C (HK1.4; Cat#48-5932-82), Ly6G (1A8; Cat#127624), I-A/I-E (M5/114.15.2; Cat# 107628), PD1 (J43; Cat# 48-9981-82), Aqua LIVE/DEAD dye (Cat#L34965). All the antibodies were purchased from the following companies: BD Bioscience (San Jose, CA, USA), eBiosciences (ThermoFisher Scientific, Waltham, MA, USA), Bio-rad Laboratories (Hercules, CA, USA) and Biolegend (San Diego, CA, USA). Samples were acquired with FACS Canto II (BD, Franklin Lakes, NJ, USA) and analyzed by FlowJo software (Tree Star, Inc., Ashland, OR, USA).

Western blot (WB)

Cell lysates were prepared in Laemmli Buffer and denatured at 100°C. Insoluble materials were removed by centrifugation. Samples were subjected to SDS-polyacrylamide 10% Tris-Glycine or Bis-Tris gel electrophoresis and blotted onto PVDF-membrane (Immobilon P membranes, Millipore, Billerica, MA, USA). Tris-buffered saline plus 0.05% Tween-20 and 5% non-fat dry milk were used to block unspecific sites. Membranes were incubated with rabbit anti-ARG1 primary antibody (H-110 clone, Santa Cruz Biotechnology Inc., Dallas, USA; Cat# sc-20150), rabbit anti-NOS2 primary antibody (Proteintech Europe, Manchester, UK; Cat# 18985-1-AP), mouse anti-TERT primary antibody, (Novus Biologicals, Centennial, CO, USA; Cat# NB100-317) and with donkey anti-rabbit or sheep anti-mouse HRP-conjugated secondary antibodies (GE Healthcare, Chicago, Illinois, USA). HRP-conjugated anti-β actin (Cell Signalling Technologies, Danvers, MA, USA; Cat# 5125) and HRP-conjugated anti-GAPDH (Cell Signalling Technologies, Danvers, MA, USA; Cat# 8884) were used as reference. Proteins were revealed by GE ImageQuant LAS400 with Femto substrate (ThermoFisher Scientific, Waltham, MA, USA; Cat# 34096).

Real-time PCR

Total RNA was isolated by TRIzol reagent (Thermo Fisher Scientific, Waltham, MA, USA; Cat# 15596018). The amount and purity of isolated RNA was analyzed by the ND-1000 Spectrophotometer (NanoDrop Technologies). cDNA was prepared using the SuperScript® cDNA Synthesis Kit (Thermo Fisher Scientific, Waltham, MA, USA; Cat# emr437050) according to the manufacturer's instruction. Real Time PCR was run using 2x SYBR Green master mix (ThermoFisher Scientific, Waltham, MA, USA; Cat# 4364346). All samples were normalized using GAPDH endogenous control primers. Post-qRT-PCR analysis to quantify relative gene expression was performed by the comparative Ct method ($2^{-\Delta\Delta Ct}$).

In vitro MDSC and BM-derived macrophages generation

Tibias and femurs were removed in sterility from C57BL/6 mice, and bone marrow cells were flushed. Red blood cells were lysed with a hypotonic solution containing 8.3% NH₄Cl, 1% KHCO₃ and 0.5M EDTA. To obtain MDSC, BM cells were cultured accordingly to recent published protocols [4]. Briefly, 1.5 x 10⁶ cells were cultured in RPMI 1640 (Euroclone, Milan, Italy) supplemented with 40 ng/mL IL-6 (Miltenyi Biotec, Bologna, Italy; Cat# 130-096-686), 40 ng/mL GM-CSF (Miltenyi Biotec, Bologna, Italy; Cat# 130-095-735), 10% heat-inactivated FBS (Superior, Merck, Darmstadt, Germany), 2mM L-glutamine, 10mM HEPES, 1mM sodium pyruvate, 150U/mL streptomycin, 200U/mL penicillin/streptomycin (all from Euroclone, Milan, Italy). Cultures were maintained at 37°C in 5% CO₂-humidified atmosphere for 4 days.

To promote macrophage differentiation, BM cells were cultured in RPMI 1640 (Euroclone, Milan, Italy) supplemented with 100ng/mL CSF-1 (Miltenyi Biotec, Bologna, Italy; Cat# 130-101-706), 10% heat-inactivated FBS (Superior, Merck, Darmstadt, Germany), 2mM L-glutamine, 10mM HEPES, 1mM sodium pyruvate, 150U/mL streptomycin, 200U/mL penicillin/streptomycin (all from Euroclone, Milan, Italy), according to already established protocols [5]. Cultures were maintained at 37°C in 5% CO₂-humidified atmosphere for 7 days. On day 4 of culture, fresh cytokine-supplemented complete medium was added. To obtain M1-Mφ or M2-Mφ, at day 7 macrophages were cultured in presence of IFN-γ (10 U/mL; Miltenyi Biotec, Bologna, Italy; Cat# 130-105-773) and LPS (1 μg/mL; Cat# L8274; Sigma-Aldrich, Saint Louis, MO, USA) or IL-4 (10 ng/mL; Miltenyi Biotec, Bologna, Italy; Cat# 130-097-758) and IL-13 (10 ng/mL; Miltenyi Biotec, Bologna, Italy; Cat# 130-096-688) cytokines-cocktail, respectively.

Metabolite profiling and quantitation

For HPLC-MS experiments, the HPLC system (Shimadzu) was coupled to a LTQ Orbitrap Velos instrument (Thermo Fisher Scientific, MA, USA) and set at 30000 resolution to acquire HPLC-MS data. An Agilent ZORBAX ODS C18 column (150 mm×2.1 mm, 3.5 μm, Agilent, USA) was used. Sample analysis was performed in positive ion modes with a spray voltage of 4.5 kV and capillary temperature of 350°C. The mass scanning was 50–1500 m/z. The flow rates of nitrogen sheath gas and nitrogen auxiliary gas were established to be the range of 30 L/min and 10 L/min, respectively. The HPLC-MS system was run in binary gradient mode. Solvent A was 0.1% (v/v) formic acid/water, and solvent B was 0.1% (v/v) formic acid/methanol. The gradient was as follows: 5% B at 0 min, 5% B at 5 min, 100% B at 8 min, 100% B at 9 min, 5% B at 18 min, and 5% B at 20 min. The flow rate was 0.2 mL/min. To ensure system equilibrium, the pooled QC sample was injected five times at the beginning. QC sample was injected every five samples during samples detection to further monitor the system stability.

Extracellular flux analysis

Oxygen consumption rate (OCR) and Extracellular Acidification Rate (ECAR) were measured in bone marrow-derived macrophages and CTLs - either untreated or previously treated with AT38 - by using a Seahorse XFe24 Extracellular Flux Analyzer (Agilent, CA, USA,). On the day of the assay, cells were seeded at the density of 1.25×10^5 cells/well (macrophages) or 3.5×10^5 cells/well (CTLs) in a V7 XFe24-well cell culture microplate coated with poly-D-lysine and centrifuged at 400 RCF for 2 minutes to attach them to the bottom of the plate. Cells were incubated in Assay Medium consisting of Seahorse XF DMEM Medium (Agilent, CA, USA, Cat# 103575-100) supplemented with 10 mM glucose, 1 mM Sodium Pyruvate, and 4mM (macrophages) or 2mM (CTLs) glutamine, pH 7.4, at 37°C in a non-CO₂ incubator for 1 hour. Mito stress test was performed measuring OCR and ECAR at the baseline and after sequentially adding 1 μ M oligomycin A, 1 μ M (macrophages) or 0.75 μ M (CTLs) of carbonyl cyanide 4-(trifluoromethoxy) phenylhydrazone (FCCP) and 0.5 μ M each of Rotenone and Antimycin A. Data were normalized to the DNA content *per* well that was quantified with the CyQUANT Cell proliferation assay kit (Thermo Fisher Scientific, MA, USA, Cat# C35007), according to the manufacturer's instructions, and analysed as described [6].

Tumour models and immunotherapy protocols

For subcutaneous (s.c.) tumour studies, 5×10^5 FC1199, FC1199-Luc, FC1242 and FC1242-Luc tumour cell lines were injected in the flank of C57Bl/6 WT mice. Tumour growth was monitored every 2 days using a digital caliper. The greatest longitudinal diameter (length) and the greatest transverse diameter (width) were determined and tumour volume was calculated by the modified ellipsoidal formula: tumour volume = $1/2$ (length \times width²). Immunotherapy treatments included 2 consecutive ACTs of 1×10^7 mTERT-specific or OVA-specific CTLs (Supplementary Figure 2C).

For the generation of orthotopic model, anesthetized mice were orthotopically injected into the exposed pancreas with tumour cells suspended in Matrigel (BD biosciences; Cat# 356234) using a 29 gauge needle, after a small 0.5 cm incision in the left abdomen was made. The peritoneum was then closed with dissolvable suture and the skin incision closed with wound clips. 5×10^4 FC1199-Luc or FC1242-Luc cells, were injected in the pancreas of WT immune competent mice whereas 5×10^5 HF2-Luc human PDAC cells were orthotopically injected in immunodeficient NOG mice. Immunotherapy included 3 consecutive ACTs of 1×10^7 mTERT₁₉₈₋₂₀₅-specific or control OVA₂₅₇₋₂₆₄-specific CTLs, or hTERT₈₆₅₋₈₇₃- or control HCV₁₄₀₆₋₁₄₁₅-specific human T cells lymphocytes for mouse or human experimental settings, respectively (Supplementary Figure 2G). 5×10^6 mTERT₁₉₈₋₂₀₅-, or OVA₂₅₇₋₂₆₄-pulsed irradiated splenocytes or 5×10^6 hTERT₈₆₅₋₈₇₃- or HCV₁₄₀₆₋₁₄₁₅-pulsed irradiated PBMCs were injected together with mouse and human TERT-specific T lymphocytes in immune competent and immune deficient mice, respectively.

8 weeks old transgenic KPC mice underwent high-resolution ultra-sound imaging to monitor autochthonous tumour development and then assigned to the treatment groups. KPC mice received an immunotherapy protocol which included an adoptive transfer/month of 1×10^7 mTERT₁₉₈₋₂₀₅-specific or control OVA₂₅₇₋₂₆₄-specific CTLs together with 5×10^6 respective peptide-pulsed irradiated splenocytes (Supplementary Figure 2I). When indicated, mice were treated with either 30 mg/kg/d of AT38 in 1% carboxymethyl cellulose/water (vehicle) or vehicle alone through a double i.p. injection each day for 7 days; ACT was provided at day 4 of treatment. In every set-up rhIL-2 (30,000 IU/mouse every 12h, for a total of 6 doses) was supplied by i.p. administration in order to sustain ACT.

Ultrasound imaging

KPC mice develops spontaneous, stepwise, multi-focal lesions that ultimately progresses to PDAC [7, 8]. We exploited high-resolution ultra sound imaging (Vevo 2100, FUJIFILM VisualSonics,

Toronto, ON, Canada) to identify the main tumour mass target of action of ACT, in order to meet enrolment criteria and to follow-up tumour evolution and objective response (OR) during treatment. We identified target lesions by taking advantage of specific anatomic landmarks: kidneys, spleen, liver, portal vein and inferior vena cava. Ultrasound sessions were performed in a blinded fashion and analysis was independently supervised by two investigators (F.D.S and C.A.). Tumour volume was estimated by measuring 2 smallest and largest perpendicular tumour dimensions (as for caliper measurements) and followed during disease progression, thus tumour volume change was calculated according to the following formula: $(V1-V0)/V0 \times 100$, where V0 and V1 are the tumour volumes measured before and after treatment, respectively.

Bioluminescence imaging

In orthotopic PDAC models, tumour growth was monitored by bioluminescence imaging (BLI; photons/second/cm²/sr) using the IVIS Spectrum Imaging System (Perkin Elmer, Waltham, MA, USA). Images were acquired prior to treatment and then weekly. Animals were anesthetized with isoflurane/oxygen. Mice were ventrally imaged before and 10 minutes after i.p. administration of D-luciferin (Perkin Elmer, Waltham, MA, USA; Cat #122799) according to vendor instructions, in order to discriminate specific light signal from basal emission. The subsequent parameters were used: exposure time = 5 minutes, field of view = 19×19 cm, binning B = 8 and f/stop = 1. Images were quantified tracing the region of interest (ROI) on the entire animal body. Living Image Software 4.4 (Perkin Elmer, Waltham, MA, USA) was used to acquire and quantify the bioluminescence.

Histopathology analysis

Pancreas and tumour samples were fixed in 10% neutral buffered formalin and embedded into paraffin or fixed in 1% PFA and frozen in a cryo-embedding medium (OCT, Bio-Optica, Milano, Italy); slides were cut and stained with Hematoxylin (Bio-Optica, Milano, Italy) and Eosin (Bio-Optica, Milano, Italy) for histological examination.

For immunohistochemical evaluation of frozen samples, sections were air-dried, fixed in ice-cold acetone for 10 min and incubated with the following primary antibodies: anti-Telomerase (Ab-2) rabbit pAb (Cat #582005, Calbiochem, Merck, Darmstadt, Germany), rat monoclonal anti-mouse CD8a antibody (Cat #550281, BD Pharmingen, San Jose, CA, USA), rat monoclonal anti-mouse CD11b antibody (Cat #550282, BD Pharmingen, San Jose, CA, USA), rabbit polyclonal anti-CD3 antibody (Cat #ab828, Abcam, Cambridge, UK), rabbit polyclonal anti-Arginase I (Cat #sc-20150, Santa Cruz Biotechnology, Dallas, TE, USA), rabbit polyclonal anti-iNOS antibody (Cat #PA3-030A, Thermo Scientific, Waltham, MA, USA), anti-Gr1 antibody (RB6-8C5, by homemade production), and rabbit polyclonal anti-Nitrotyrosine antibody (Cat #06-284, Millipore, Merck, Darmstadt, Germany), followed by the appropriate secondary antibodies (Jackson ImmunoResearch Laboratories, Cambridgeshire, UK). For immunohistochemistry of paraffin-embedded samples, slides were deparaffinized, serially rehydrated and, after the appropriate antigen retrieval procedure, stained with monoclonal mouse anti-human CD8 (Cat #M7103, Dako, Agilent, Santa Clara, CA, USA), polyclonal rabbit anti-Nitrotyrosine antibody (Cat #06-284, Millipore, Merck, Darmstadt, Germany), FLEX monoclonal mouse anti-human CD15 antibody (Cat #GA06261-2, Dako, Agilent, Santa Clara, CA, USA), rabbit polyclonal anti-Arginase I antibody (Cat #sc-20150, Santa Cruz Biotechnology, Dallas, TE, USA), mouse anti human CD68 antibody (Cat #M0814, Dako, Agilent, Santa Clara, CA, USA) followed by the appropriate secondary antibodies. Immunoreactive antigens were detected using streptavidin peroxidase (Thermo Scientific, Waltham, MA, USA) and the DAB Chromogen System (Dako, Agilent, Santa Clara, CA, USA) or alkaline phosphatase conjugated streptavidin (Thermo Scientific, Waltham, MA, USA) and Vulcan fast red Chromogen (Biocare Medical, Pacheco, CA, USA). After chromogen incubation, slides were counterstained in

Hematoxylin (Bio-Optica, Milano, Italy) and images were acquired by Leica DMRD optical microscope (Leica, Wetzlar, Germany). For histological assessment of collagen deposition, trichrome staining was performed using the Masson Trichrome with Aniline Blue Staining Kit (04-010802, Bio-Optica, Milano, Italy).

scRNA-sequencing

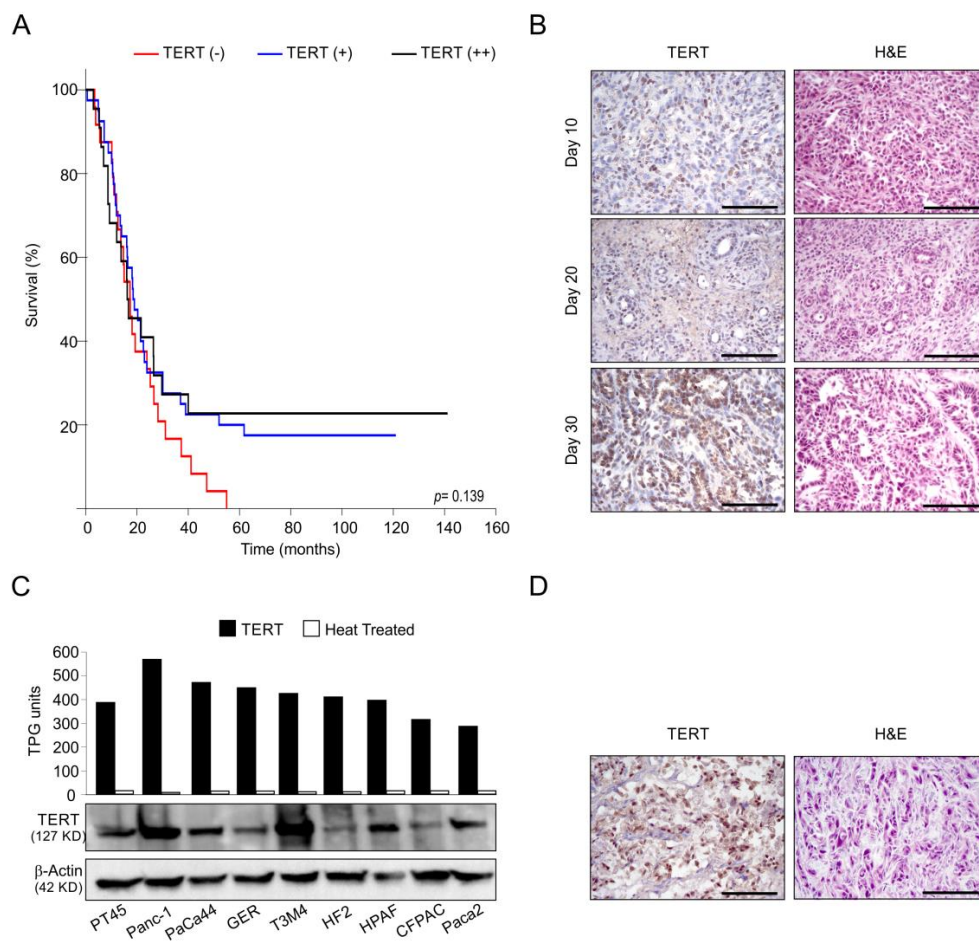
Mice bearing 7-days orthotopic FC1242 tumours, were treated with either 30 mg/kg/d of AT38 in 1% carboxymethyl cellulose/water (vehicle) or vehicle alone through a double i.p. injection each day for 7 days as indicated above. Mice were sacrificed, tumours isolated and processed in order to obtain cell suspensions. Two samples/group (each one composed by a pool of 4 mice), were enriched for CD45 marker on FACS ARIA (BD biosciences) instrument. FACS-sorted cells were resuspended in RPMI with 5% FBS to a final concentration of 1000 cells per ml and processed using the 10x Genomics Chromium Controller and the Chromium NextGEM Single-Cell 3' GEM, Library & Gel Bead kit v3.1 (Pleasanton, California, United States) following the standard manufacturer's instructions [9]. ScRNA-seq data was processed using the 10x Cell Ranger software (v.3.1.0) (<http://software.10xgenomics.com/single-cell/overview/welcome>) and aligned to the mouse reference genome (mm10). Prior to integration and cell type identification, barcode matrices were inspected for quality control. In particular, Scrublet (v0.2.1) software [10] was used to remove putative doublets, setting a threshold of 0.53 looking at the histograms of doublet scores generated by the software. In addition, a filtering step was performed using the Seurat (v3.1.5) R package [11] in order to keep high quality cells based on the mitochondrial gene expression percentage (<20%), minimum/maximum number of expressed genes (>250 and <7,500) and minimum/maximum gene counts (>500 and <100,000). After log-normalization, barcode matrices were integrated using the standard Seurat method [11] with 30 dimensions of the canonical correlation analysis (CCA). Subsequently, integrated data was scaled regressing for the number of expressed genes, counts and percentage of mitochondrial gene expression. The top 2,000 variable genes obtained from the 'vst' procedure of Seurat were employed for principal component analysis (PCA). The first 19 principal components were used to project the cells into a 2-dimensional space using Uniform Manifold Approximation and Projection (UMAP). Automatic cell type classification was performed with SingleR [12] using as reference dataset the gene signatures from the Immunological Genome Project (<https://www.immgen.org>). After classification, only immune cells were kept and the expression of known immunological marker genes was checked through diagnostic plots. Despite quality control, a closer inspection revealed few cells expressing both myeloid (*Cd68*) and lymphocyte (*Cd3d*) markers that were removed from further analyses because containing potential doublets. Gene set enrichment analysis (GSEA) for cell populations was performed using the R package fgsea [13] with the 50 hallmark gene sets from MSigDB [14]. Differential gene expression analysis was obtained using the Wilcoxon Rank Sum test of Seurat with average log-fold change threshold of 0. Up- or down-regulated genes and gene sets with an adjusted p-value < 0.05 were considered statistically significant. The conversion from mouse to human gene symbols was performed using the biomaRt (v.2.42.0) R package [15].

REFERENCES:

- 1 Mennuni C, Ugel S, Mori F, Cipriani B, Iezzi M, Pannellini T, *et al.* Preventive vaccination with telomerase controls tumor growth in genetically engineered and carcinogen-induced mouse models of cancer. *Cancer Res* 2008;**68**:9865-74.
- 2 Sandri S, Bobisse S, Moxley K, Lamolinara A, De Sanctis F, Boschi F, *et al.* Feasibility of Telomerase-Specific Adoptive T-cell Therapy for B-cell Chronic Lymphocytic Leukemia and Solid Malignancies. *Cancer Res* 2016;**76**:2540-51.
- 3 Facciabene A, De Sanctis F, Pierini S, Reis ES, Balint K, Facciponte J, *et al.* Local endothelial complement activation reverses endothelial quiescence, enabling t-cell homing, and tumor control during t-cell immunotherapy. *Oncoimmunology* 2017;**6**:e1326442.
- 4 Solito S, Pinton L, De Sanctis F, Ugel S, Bronte V, Mandruzzato S, *et al.* Methods to Measure MDSC Immune Suppressive Activity In Vitro and In Vivo. *Curr Protoc Immunol* 2019;**124**:e61.
- 5 Marigo I, Trovato R, Hofer F, Ingangi V, Desantis G, Leone K, *et al.* Disabled Homolog 2 Controls Prometastatic Activity of Tumor-Associated Macrophages. *Cancer Discov* 2020;**10**:1758-73.
- 6 Bifari F, Dolci S, Bottani E, Pino A, Di Chio M, Zorzini S, *et al.* Complete neural stem cell (NSC) neuronal differentiation requires a branched chain amino acids-induced persistent metabolic shift towards energy metabolism. *Pharmacol Res* 2020;**158**:104863.
- 7 Dugnani E, Pasquale V, Marra P, Liberati D, Canu T, Perani L, *et al.* Four-class tumor staging for early diagnosis and monitoring of murine pancreatic cancer using magnetic resonance and ultrasound. *Carcinogenesis* 2018;**39**:1197-206.
- 8 Hingorani SR, Wang L, Multani AS, Combs C, Deramaudt TB, Hruban RH, *et al.* Trp53R172H and KrasG12D cooperate to promote chromosomal instability and widely metastatic pancreatic ductal adenocarcinoma in mice. *Cancer Cell* 2005;**7**:469-83.
- 9 Bost P, De Sanctis F, Cane S, Ugel S, Donadello K, Castellucci M, *et al.* Deciphering the state of immune silence in fatal COVID-19 patients. *Nat Commun* 2021;**12**:1428.
- 10 Wolock SL, Lopez R, Klein AM. Scrublet: Computational Identification of Cell Doublets in Single-Cell Transcriptomic Data. *Cell Syst* 2019;**8**:281-91 e9.
- 11 Butler A, Hoffman P, Smibert P, Papalexi E, Satija R. Integrating single-cell transcriptomic data across different conditions, technologies, and species. *Nat Biotechnol* 2018;**36**:411-20.
- 12 Aran D, Looney AP, Liu L, Wu E, Fong V, Hsu A, *et al.* Reference-based analysis of lung single-cell sequencing reveals a transitional profibrotic macrophage. *Nat Immunol* 2019;**20**:163-72.
- 13 Korotkevich G, Sukhov V, Budin N, Shpak B, Artyomov MN, Sergushichev A. Fast gene set enrichment analysis. *bioRxiv* 2021:060012.
- 14 Liberzon A, Birger C, Thorvaldsdottir H, Ghandi M, Mesirov JP, Tamayo P. The Molecular Signatures Database (MSigDB) hallmark gene set collection. *Cell Syst* 2015;**1**:417-25.
- 15 Durinck S, Moreau Y, Kasprzyk A, Davis S, De Moor B, Brazma A, *et al.* BioMart and Bioconductor: a powerful link between biological databases and microarray data analysis. *Bioinformatics* 2005;**21**:3439-40.

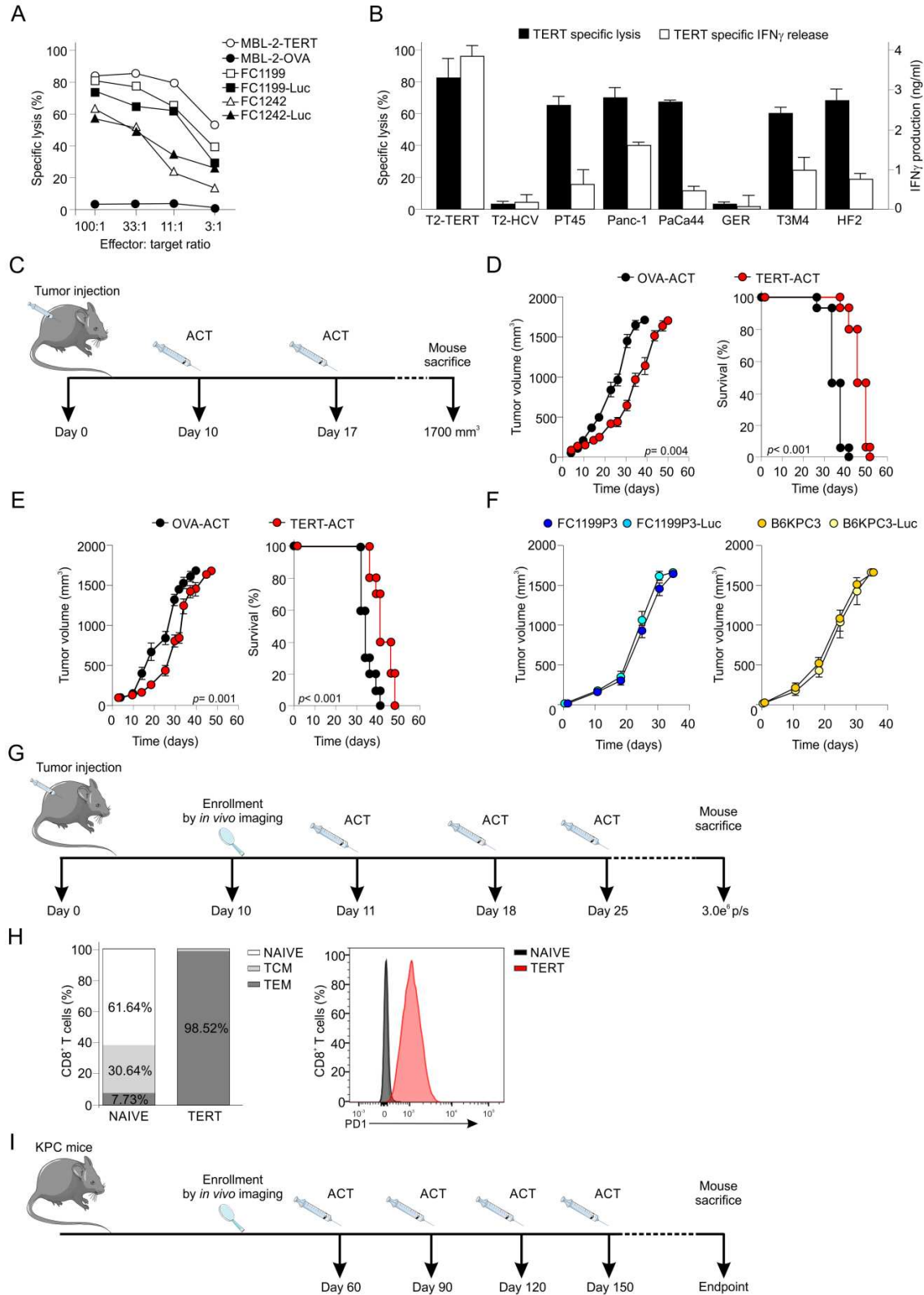
Supplementary Figures:

Supplementary Figure 1



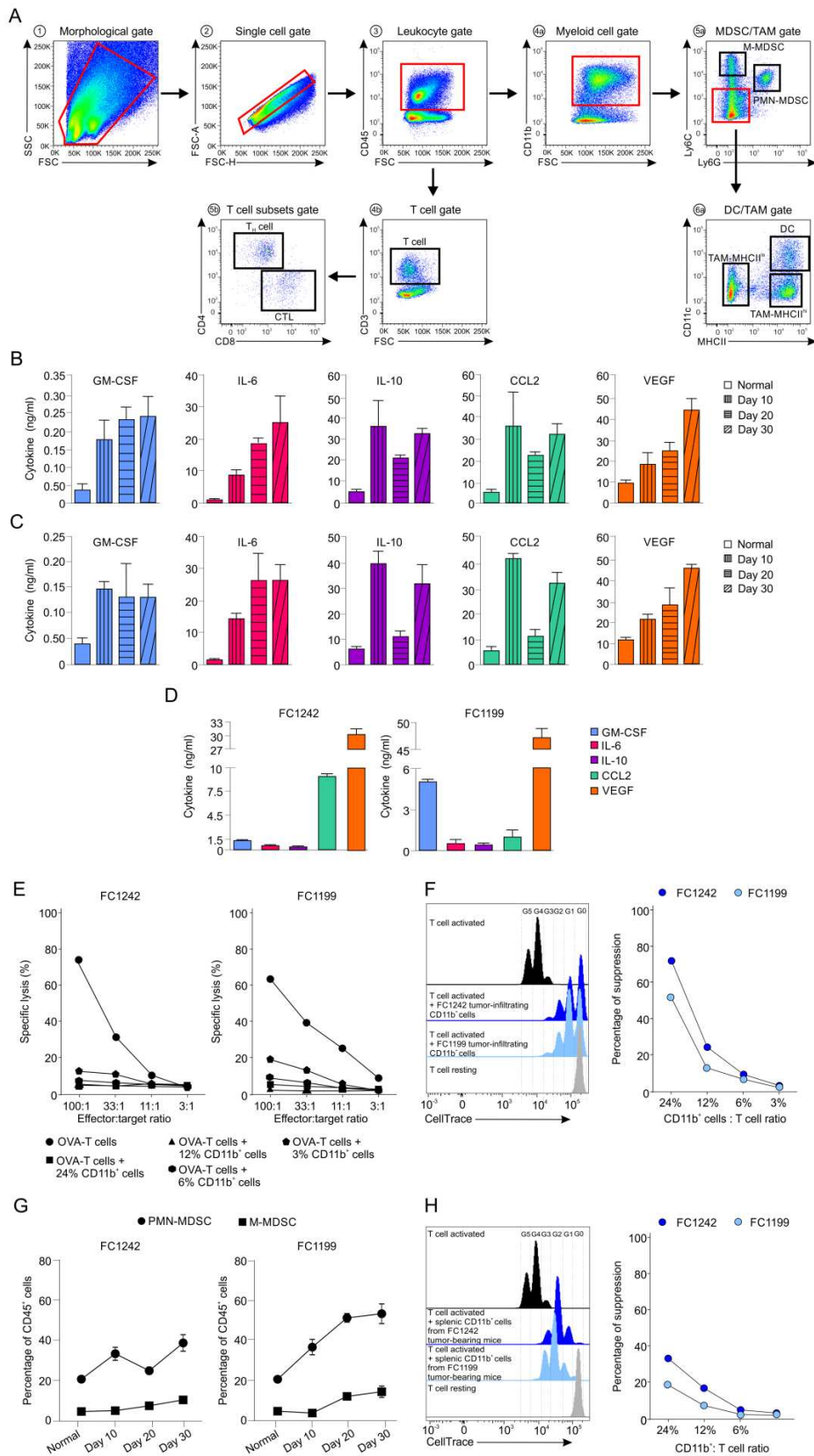
Supplementary Figure 1. TERT detection in PDAC tissues. A) Kaplan–Meier curves for overall survival (OS) in PDAC patients (n =88) by TERT expression. Survival curves were compared by Mantel-Haenszel (long-rank) test. B) Representative TERT IHC analysis (left panel) and H&E staining (right panel) in tumours isolated from C57BL/6 mice orthotopically injected with FC1199 cells and sacrificed at different time points (ten to thirty days) from tumour challenge. C) TERT activity and expression in several human PDAC cell lines by TRAP assay (top panel; untreated samples, black; heat-inactivated samples, white) and Western blot (WB, bottom panel), respectively. Representative samples are shown. D) Representative TERT IHC analysis (left panel) and H&E staining (right panel) in human HF2 PDAC cell line-derived orthotopic xenograft isolated from immunodeficient mice. Scale bar, 100 μ m (B, D).

Supplementary Figure 2



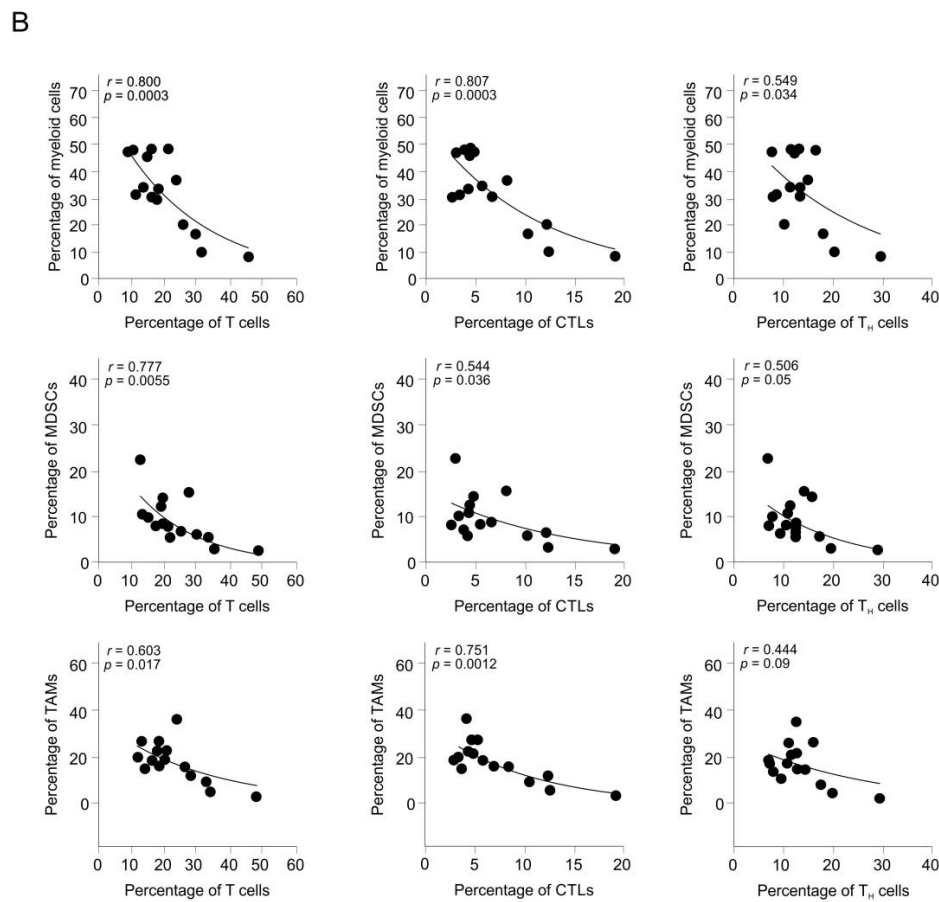
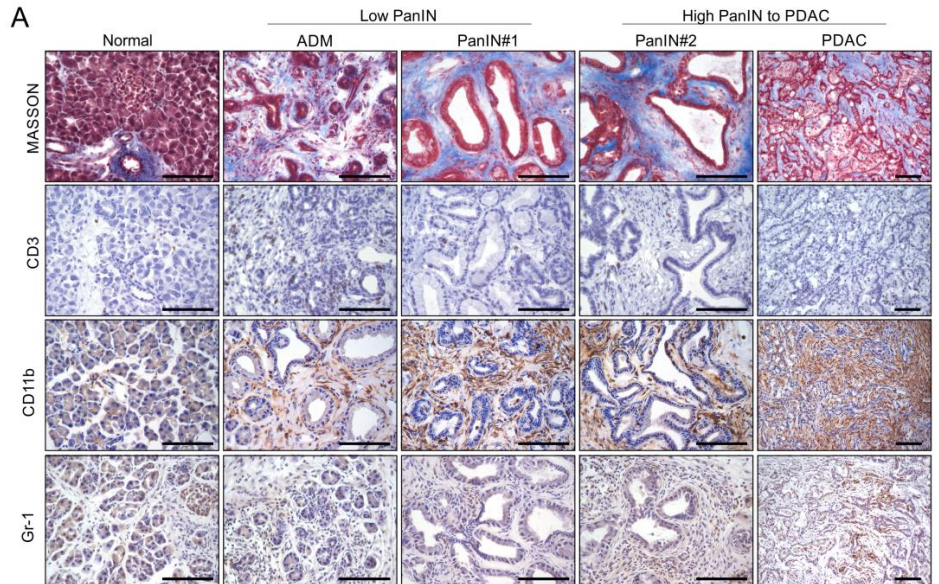
Supplementary Figure 2. TERT immunotherapy in PDAC tumour-bearing mice. A) Cell killing activity of mTERT₁₉₈₋₂₀₅-specific mouse T lymphocytes was evaluated by ⁵¹Cr release assay. MBL-2 (H-2^b mouse leukaemia cell line) pulsed with OVA₂₅₇₋₂₆₄- or mTERT₁₉₈₋₂₀₅-peptides were used as negative and positive target controls, respectively, to prove the specific killing ability of mTERT₁₉₈₋₂₀₅-specific mouse CTLs. A representative experiment of three replicates is shown. B) Functional activity of hTERT₈₆₅₋₈₇₃-specific, engineered human T lymphocytes was evaluated by ⁵¹Cr release assay (black bars, expressed as %, left axis) and IFN γ release (white bars, indicated as ng/ml, right axis). T2 (HLA-A2⁺, human lymphoblast cell line) pulsed with hHCV₁₄₀₆₋₁₄₁₅ or hTERT₈₆₅₋₈₇₃ peptides were used as negative and positive target controls, respectively, to prove the specific killing and activation (IFN γ release) ability of hTERT₈₆₅₋₈₇₃-specific human CTLs. Data are reported as mean \pm SD of three independent experiments. C) Schematic representation of immunotherapy administered to immunocompetent mice bearing s.c. tumours. Tumour-bearing mice received iv TERT-specific or OVA-specific CD8⁺ T lymphocytes. Therapeutic efficacy of TERT-based ACT in mice bearing s.c. FC1242- (D) or FC1199- derived tumours (E) evaluated as tumour growth (left panel) and overall survival (right panel). Tumour growth data are reported as mean \pm SE of a representative experiment of three independent replicates; OVA-ACT (n=8) and TERT-ACT (n=8). Statistical analysis was performed using one-way analysis of variance (ANOVA) and Mantel-Haenszel (long-rank) test respectively. F) *In vivo* s.c. tumour growth of FC1199-Luc, FC1242-Luc or WT counterparts in C57Bl/6 mice. G) Schematic representation of immunotherapy administered to immunocompetent mice bearing orthotopic tumours shown in Figure 2A, 2B and 2E. Tumour-bearing mice received iv TERT-specific or OVA-specific CD8⁺ T lymphocytes. H) T lymphocytes isolated from naïve spleen mouse and cultured TERT-specific CTLs were analysed according to the expression of differentiation (CD44, CD62L, left panel) and exhaustion (PD1, right panel) markers and classified as naïve (CD62L⁺, CD44⁻), T central memory (TCM, CD62L⁺ CD44⁺), T effector memory (TEM, CD62L⁻, CD44⁺). I) Schematic representation of immunotherapy administered to KPC mice enrolled at 8 weeks of age in either TERT-ACT (n=20) or OVA-ACT (n=20) experimental groups. Tumour-bearing mice received iv TERT-specific or OVA-specific CD8⁺ T lymphocytes.

Supplementary Figure 3



Supplementary Figure 3. Characterization of myeloid cell subsets and tumour cells during pancreatic cancer evolution. A) Representative gating strategy of flow cytometry to identify tumour-infiltrating myeloid cells in PDAC specimens isolated from either KPC or C57Bl/6 mice orthotopically engrafted with KPC-derived cell lines (5×10^4 FC1199-Luc or FC1242-Luc). B-C) Cytokine profile of tumour specimens isolated from FC1242 (B) or FC1199 (C) tumours at different stages of PDAC progression (ten to thirty days since tumour challenge) obtained by a 24h *in vitro* cell culture of homogenized tumours. D) Cytokine profile of KPC-derived cell lines, after 24h of *in vitro* cell culture. Data are reported as mean \pm SD of three independent experiments (C, D). E-F) CD11b⁺ cells isolated from FC1242 and FC1199 tumours were incubated at different cell proportion with antigen activated OT-1 splenocytes. After 5 days of co-culture, MLPCs were tested in a cytotoxicity test by ⁵¹Cr release assay against OVA₂₅₇₋₂₆₄ peptide- or β -gal₉₆₋₁₀₃ peptide-pulsed cells (E) or CD11b⁺ cells were incubated at different cell proportion with antigen activated cell trace-labeled OT-1 splenocytes in order to evaluate the ability to suppress their proliferation (F). Cell Trace dilution representative plots are shown in left panels. G) Frequency of M-MDSC (CD11b⁺ Ly6C⁺ Ly6G⁻) and PMN-MDSC (CD11b⁺ Ly6C^{-low} Ly6G⁺) cell subsets in spleen of PDAC tumour-bearing mice (ten to thirty days since tumour challenge). H) Suppressive activity of spleen derived CD11b⁺ cells isolated from either FC1242- or FC1199- tumour bearing mice was evaluated by measuring OVA-activated Cell Trace-labeled CD8⁺ T lymphocytes proliferation. Cell Trace dilution representative plots are shown in left panels. A representative experiment of three independent replicates is shown (E, F, H).

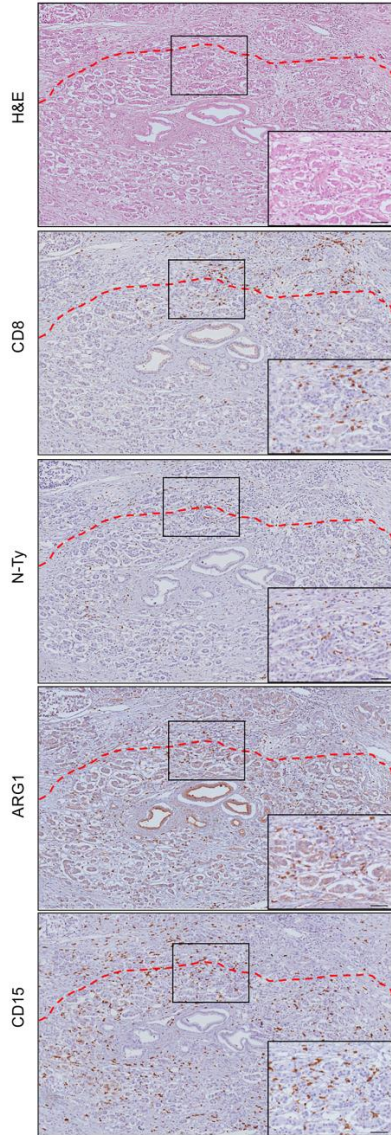
Supplementary Figure 4



Supplementary Figure 4. Immune characterization of PDAC evolution in KPC mice. A) Representative IHC analysis to monitor ECM deposition (Masson Trichrome), T lymphocytes (CD3), myeloid (CD11b) and MDSCs (Gr-1) infiltration in KPC tumour specimens at different stage of PDAC progression. Scale bar, 100 μ m. B) Spearman's rank correlation of cell frequency between tumour-infiltrating myeloid cells (CD11b⁺ cells) or MDSCs (CD11b⁺ Ly6C⁺ Ly6G⁻ M-MSDCs plus CD11b⁺ Ly6C^{-/low} Ly6G⁺ PMN-MDSCs) or TAMs (Ly6C⁻ Ly6G⁻ CD11c⁻ MHCII⁺ F4/80⁺ TAM MHCII^{high} plus Ly6C⁻ Ly6G⁻ CD11c⁻ MHCII⁻ F4/80⁺ TAM MHCII^{low}) and T lymphocytes (CD3⁺ cells) or CTLs (CD3⁺CD8⁺ cells) or T_H (CD3⁺CD4⁺ cells) lymphocytes.

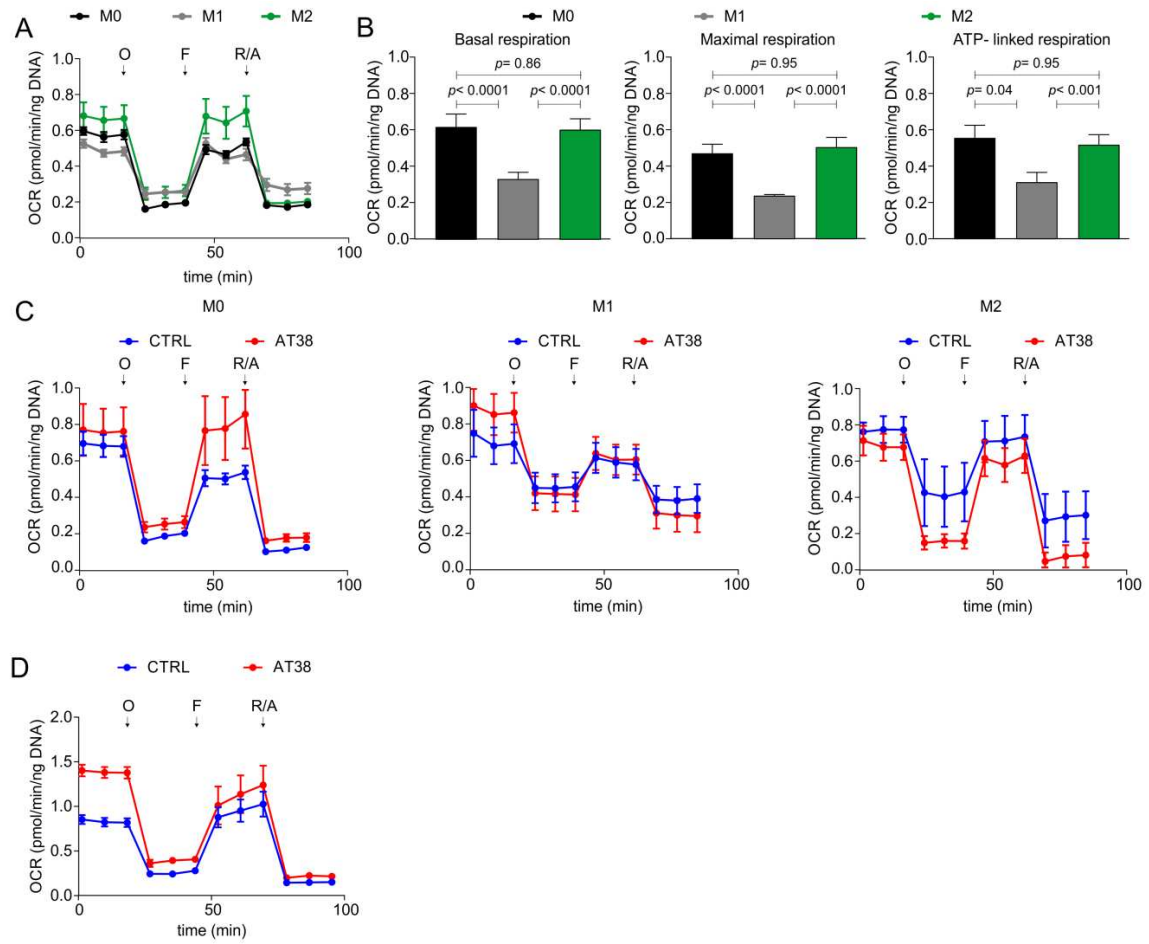
Supplementary Figure 5

A



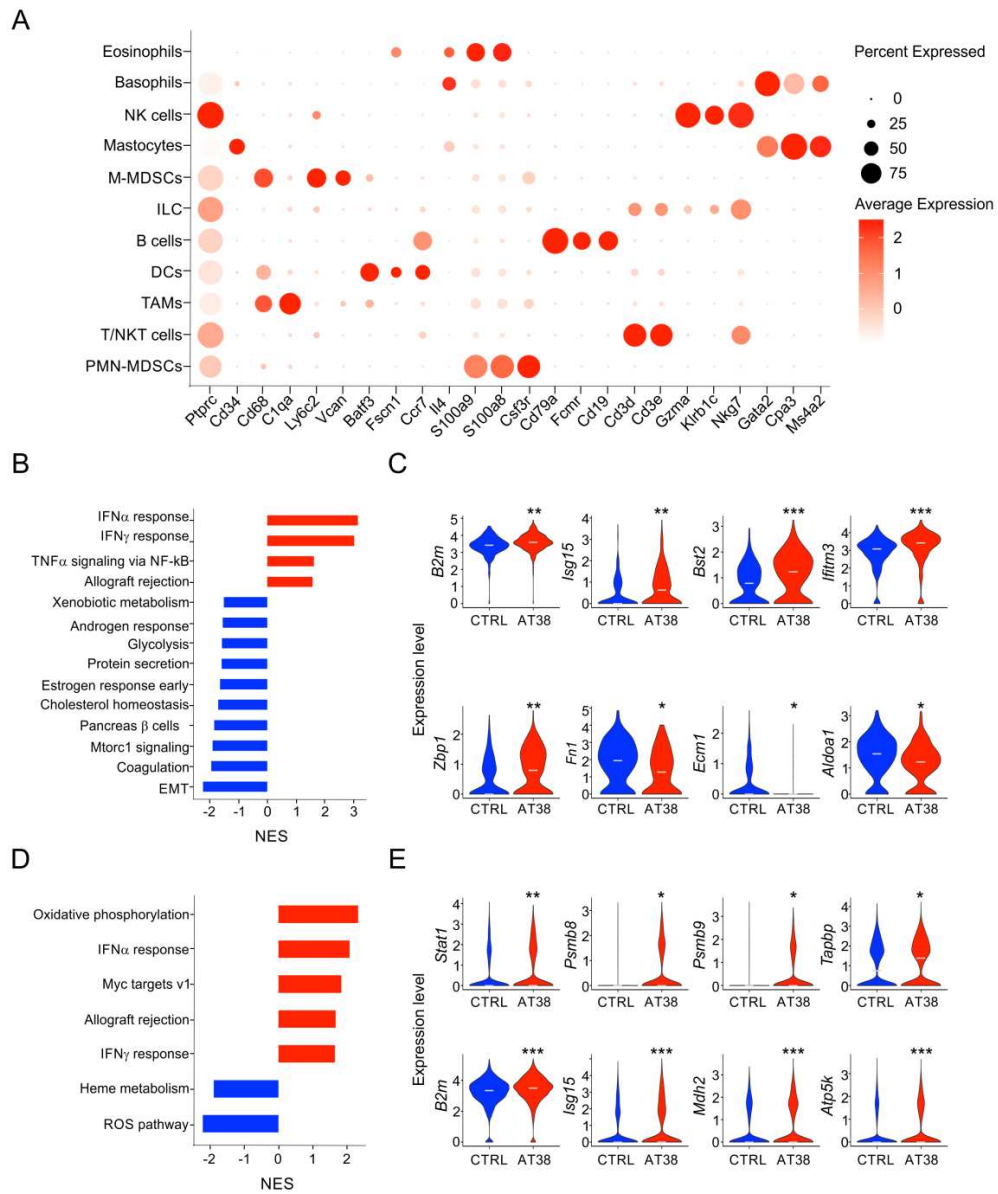
Supplementary Figure 5: NTy-based deposition occurs in tumour stroma. A) Representative IHC staining for CD8, N-Ty, ARG1 and CD15 in human PDAC tissues to evaluate the presence and localization of CTLs, RNS, ARG1 and neutrophils, respectively. Scale bar, 100 μ m.

Supplementary Figure 6



Supplementary Figure 6: AT38 reprograms the energetic metabolism of both macrophages and CTLs. A) OCR real-time changes of BM-derived M0-, M1- and M2-polarised M ϕ were assessed by Seahorse XFe24 extracellular flux analyser. O = oligomycin, F = FCCP, R/A = rotenone and Antimycin A injections. B) Quantitative analysis of respiratory parameters: basal, maximal and ATP-linked respiration. C) *In vitro* BM-derived M0-, M1- and M2-polarized macrophages were treated with AT38 (5 μ M, 24 hours). D) OCR real-time changes of *in vitro* differentiated CTLs treated or not with AT38 (5 μ M, 48 hours). Data are represented as mean \pm SEM, n = 3 biological and at 10 technical replicates.

Supplementary Figure 7

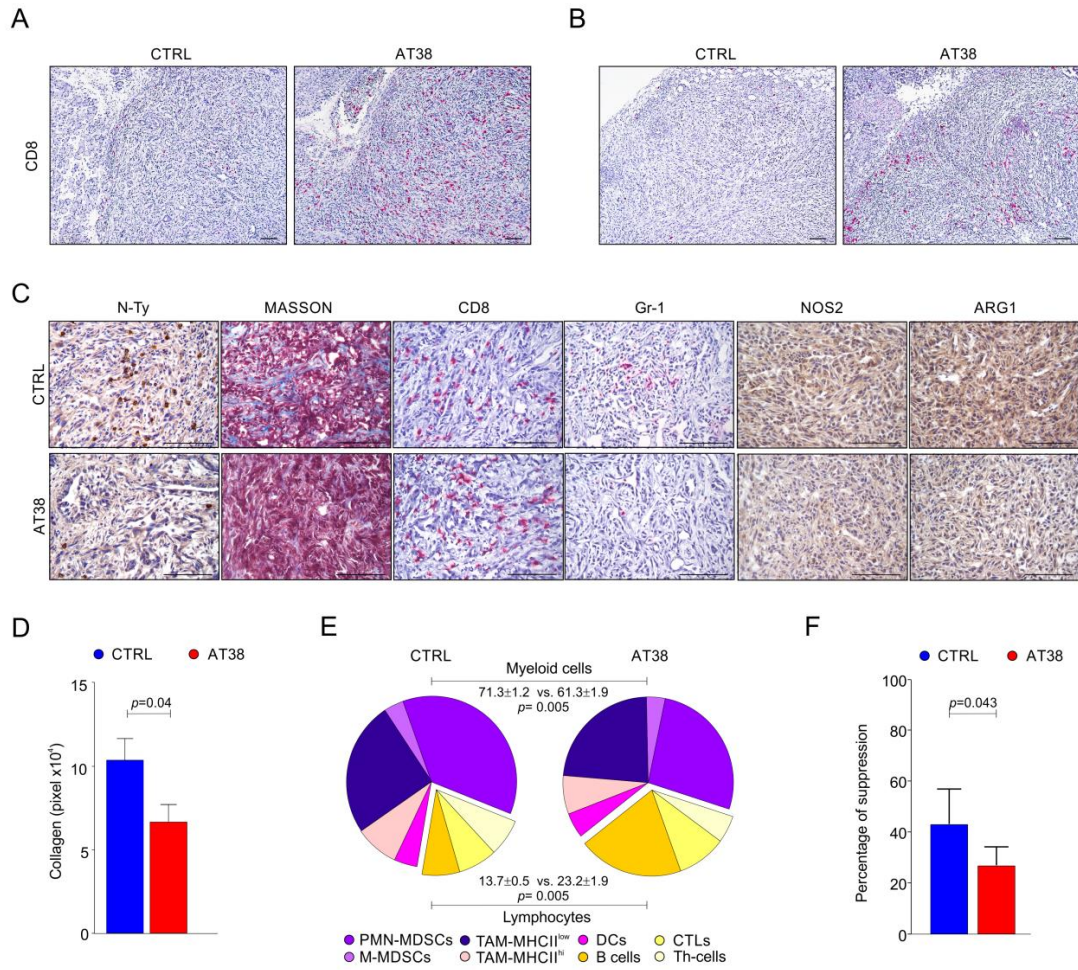


Supplementary Figure 7. AT38-dependent reprogramming of monocyte and neutrophil landscape in FC1242 tumours.

A) Dot plot showing the scaled average expression of known immunological marker genes of the identified cell populations. B) GSEA analysis with the up-(red) or down-regulated (blue) hallmark gene sets obtained comparing the M-MDSCs in mice treated with AT38. C) Violin plots showing the expression of genes involved in interferon (IFN) α/γ response (top panel), Mtorc1 signalling, and promoting tumour epithelial to mesenchymal transition (EMT, lower panel). D) GSEA analysis with the up- up-(red) or down-regulated (blue) hallmark gene sets obtained comparing the PMN-MDSCs in mice treated with AT38. E) Violin plots showing the expression of genes involved in interferon α/γ (IFN) response and oxidative phosphorylation (*p < 0.05, **p < 0.01, ***p < 0.001).

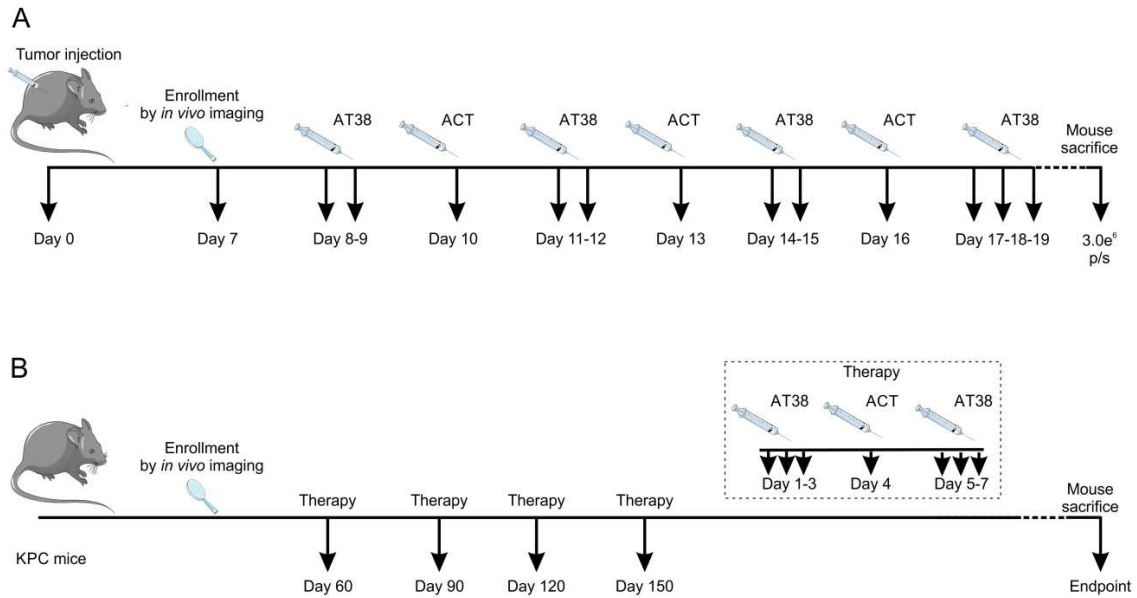
Supplementary Figure 8

Supplementary Figure 8



Supplementary Figure 8. AT38 shapes PDAC TME. A-B) Low magnification IHC staining for CTLs (CD8) in FC1242 (A) and FC1199 (B) tumour samples obtained from mice either treated or not with AT38 for 7 days. C) Tumour samples obtained from immunocompetent mice orthotopically challenged with FC1199 tumour cells, either treated or not with AT38 for 7 days were subjected to IHC analysis to monitor RNS production (N-Ty), ECM deposition (Masson Trichrome), CTLs (CD8) and MDSCs (Gr-1) tumour infiltration, and the presence of NOS2 and ARG1 enzymes. D) Quantification of collagen deposition in tumour specimens of AT38-treated or untreated FC1199 tumour-bearing mice. E) Tumour samples obtained from immunocompetent mice orthotopically challenged with FC1199 tumour cells, either treated or not with AT38 for 7 days (n=6 mice/group) were subjected to multi parametric immune phenotype analysis with the following markers: B220, CD3, CD4, CD8, CD11b, CD11c, CD45, F4/80, Ly6C, Ly6G, MHCII. F) Suppressive activity of tumour-infiltrating CD11b⁺ cells purified from CTRL or AT38 treated FC1242 tumour-bearing mice. Plot shows suppression at 24% CD11b⁺ cells co-cultured with T lymphocytes. Data are reported as mean \pm SE of three independent replicates. Statistical analysis was performed using one-way analysis of variance (ANOVA) test. Scale bar, 100 μ m (A-C).

Supplementary Figure 9



Supplementary Figure 9. Development of a combined treatment based on ACT and AT38 administration. A) Schematic representation of immunotherapy administered to immunocompetent mice bearing orthotopic FC1242_Luc tumours shown in Figure 7A. B) Schematic representation of immunotherapy administered to KPC mice shown in Figure 7B, 7C. Tumour-bearing mice received TERT-specific or OVA-specific CD8⁺ T lymphocytes iv and AT38 ip.